Available online at www.sciencedirect.com
SCIENCE DIRECT®
Inorganica Chimica Acta 357 (2004) 451–460
Inorganica Chimica Acta
www.elsevier.com/locate/ica

Synthesis, crystalline structure and photoluminescence investigations of the new trivalent rare earth complexes (Sm^{3+}, Eu^{3+} and Tb^{3+}) containing 2-thiophenecarboxylate as sensitizer

Ercules E.S. Teotonio [a], Maria Cláudia F.C. Felinto [b], Hermi F. Brito [a,*], Oscar L. Malta [c], Antônio C. Trindade [a], Renato Najjar [a], Wieslaw Strek [d]

[a] *Departamento de Química Fundamental, Instituto de Química da Universidade de São Paulo, São Paulo-SP 05508-900, Brazil*
[b] *Instituto de Pesquisas Energéticas e Nucleares Travessa R 400 Cidade Universitária, São Paulo-SP, CEP 05508-970, Brazil*
[c] *Departamento de Química Fundamental CCEN, Universidade Federal de Pernambuco, Recife-PE 50670-901, Brazil*
[d] *Institute of Low Temperature and Structure Research, PAS, 2 Okolna, Wroclaw, Poland*

Received 2 April 2003; accepted 17 August 2003

Abstract

New complexes with the general formula $[RE(TPC)_3 \cdot (H_2O)_2]$, where RE = Eu^{3+}, Sm^{3+}, Gd^{3+}, Tb^{3+} and TPC = 2-thiophenecarboxylate, have been prepared and investigated by photoluminescence spectroscopy. These compounds were characterized by complexometric titration, elemental analyses and infrared spectroscopy. The X-ray crystal structure has been determined for the $[Eu(TPC)_3 \cdot (H_2O)_2]$ compound, indicating that this complex is in dimeric form bridged by two carboxylate ions with monoclinic crystal system and space group $P2_1/n$. The coordination polyhedron can be described as a distorted square antiprism, where six oxygen atoms belong to the TPC ligand and two oxygen atoms belong to the water molecules, with site symmetry close to C_{2v}. The theoretical value of the intensity parameter Ω_2, which is in agreement with the experimental one, indicates that the Eu^{3+} ion is in a highly polarizable chemical environment. Based on the luminescence spectra, the energy transfer from the ligand triplet state (T) of TPC to the excited levels of the Eu^{3+} ion is discussed. The emission quantum efficiency of the $^5D_0$ emitting level of the Eu^{3+} ion was also determined. In the case of the Tb^{3+} ion, the photoluminescence data show the high emission intensity of the characteristic transitions $^5D_4 \rightarrow {}^7F_J$ ($J = 0$–6), indicating that the TPC ligand is a good sensitizer. It is also noticed that the complexes with the Eu^{3+} and Tb^{3+} ions are more luminescent than the complex with the Sm^{3+} ion.

Keywords: Trivalent rare earths; 2-Thiophenecarboxylate; Crystalline structures; Photoluminescence; Energy transfers

1. Introduction

The study of the coordination compounds of the trivalent rare earth ions (RE^{3+}) continues to be an active research area, which may be attributed to the luminescent properties of these compounds and their applications as optical signal amplifiers, electroluminescent devices and luminescent probes in biological systems [1–4]. The intraconfigurational 4f–4f transitions are parity forbidden and their emission and absorption spectra exhibit weak intensity under excitation monitored on the $^{2S+1}L_J$ levels of the RE^{3+} ion. However, some organic ligands in coordination compounds can act as an ''antenna'', absorbing and transferring energy efficiently to the rare earth ion and consequently increasing their luminescence yield [5].

The luminescent RE^{3+}-complexes containing the carboxylate anion as ligands have been extensively reported [6–11]. Additionally, carboxylate ligands show strong interest in the investigation of the coordination

* Corresponding author. Tel.: +55-11-3091-3708; fax: +55-11-3091-5579.
E-mail address: hefbrito@iq.usp.br (H.F. Brito).

0020-1693/$ - see front matter © 2003 Elsevier B.V. All rights reserved.
doi:10.1016/j.ica.2003.08.009

mode of the ligand–metal bond [12]. In particular, the 2-thiophenecarboxylic acid (HTPC) has been intensively studied in biological systems, which inhibit metabolically mediated calcium transfer out of bone and thus reduce the process of bone resorption [13]. Organometallic complexes of 2-thiophenecarboxylate (TPC) and their five-membered heterocyclic derived with niobium, tantalum, zirconium and titanium have been synthesized and their anticancer effects have been studied [14,15]. The metal–ligand interactions (M–TPC), where M are the metals of the 3d series, have been studied by potentiometric titration and spectroscopic methods by Sandhu et al. [16]. The 2-thiophenecarboxylate ligand has shown to be a very efficient complexing agent. An interesting characteristic of the TPC and their derivate ligands is the presence of three possible sites of coordination (two carboxylic oxygen atoms and one heterocyclic sulfur). Uranil (IV) and thorium (IV) complexes containing this ligand were investigated by Singh et al. [17]. They suggested that the coordination to the metal ions occurs via carboxylic oxygen atoms with normal bridging. Based on the infrared spectroscopy the metal–ligand interaction through the heterocyclic sulfur atom has also been observed.

The special attention given to the Eu^{3+} ion ($4f^6$) lies in the fact that its compounds generally present very intense luminescence in the red region (~615 nm), and in the reasonably large gaps between the main emitting levels and acceptor levels that are at least 12,000 cm^{-1}. Besides, from the emission and excitation spectra of the compounds containing europium ions more information about ligand-field splitting, energy transfer processes and quantum efficiency of the emitting levels can be obtained. The main emitting level ($^5D_0$) is non-degenerate, which is not split in any site symmetry [18]. In contrast to the Eu^{3+} ion, detailed analyses of the energy level structure and site of symmetry around the Tb^{3+} ion are complicated since the $^5D_4$ emitting level is ninefold degenerate. The luminescence spectra of the compounds of Tb^{3+} ion ($4f^8$ configuration) generally exhibit green color (~550 nm) in the presence of UV radiation [19].

Although photoluminescent properties of the Sm^{3+} ion (f^5 configuration) are less studied than trivalent europium and terbium ions, its compounds have shown intense luminescence of orange color [20]. The emitting $^4G_{5/2}$ state of the Sm^{3+} ion (~500 nm) is resonant with a great number of triplet states (T) of several organic ligands, which allowed an efficient energy transfer from ligand to rare earth ion ($T \rightarrow Sm^{3+}$) [21].

This paper reports on the synthesis, characterization, crystalline structure and photoluminescence properties of the new trivalent rare earth complexes (RE^{3+} = Sm, Eu and Tb) with the TPC ligand. Based on the crystalline structure of the $[Eu(TPC)_3 \cdot (H_2O)_2]$ complex, the intensity parameters were calculated and compared with the experimental ones. The energy transfer process from the triplet state (T) of TPC to the Eu^{3+} ion, radiative and non-radiative rates and experimental emission quantum efficiency were also investigated.

2. Experimental

2.1. Reagents

Ethanol and 2-thiophenecarboxylic acid were purchased from Aldrich Co. and used as received. The sodium 2-thiophenecarboxylate was prepared by dissolving the 2-thiophenecarboxylic acid in dilute NaOH solution. The water was evaporated to yield white crystals, which were dried under vacuum.

The rare earth compounds were synthesized from a mixture of four equivalents of sodium 2-thiophenecarboxylate (1 g, 6.7×10^{-3} mol) dissolved in 20 ml of ethanol and one equivalent of $EuCl_3 \cdot 6H_2O$ (0.61 g, 1.7×10^{-3} mol) in 10 ml aqueous solution. A white precipitate was formed, which was filtered, washed with distillated water to remove the excess of ligand and dried in a vacuum desiccator yielding 0.76 g (80%) of the RE-complex.

2.2. Apparatus

The carbon and hydrogen percentages in the complexes were determined from elemental analyses, using a Perkin–Elmer Model 240 microanalyzer, while the RE^{3+} content was performed by complexometric titration with EDTA [22]. The infrared absorption spectra were recorded in KBr pellets on a Bomen Model MB-102 spectrophotometer in the range of 400–4000 cm^{-1}.

X-ray crystallography data were collected on an Enraf-Nonius CAD4 Mach3 single crystal diffractometer with graphite-monochromated Mo Kα radiation (λ = 0.71073 Å) at 298 K. The orientation matrix and cell dimensions were determined by least-square refinement of the angular positions of 25 reflections. Data were processed on a Pentium PC and corrected for absorption and Lorentz polarization effects. The structure of the $[Eu(TPC)_3 \cdot (H_2O)_2]$ complex was solved by the standard Patterson heavy atom method, followed by normal difference Fourier technique. Space group, structure solution, refinement, molecular graphics and geometrical calculation have been carried out with the SHELXL97 [23] and ZORTEP [24] programs.

The excitation and emission spectra at room (~298 K) and liquid nitrogen temperature were collected at an angle of 22.5° (front face) in a spectrofluorimeter (SPEX-Fluorolog 2) with double grating 0.22 m monochromator (SPEX 1680), and a 450 W Xenon lamp as excitation source. The luminescence decay curves of the emitting levels were measured using a phosphorimeter SPEX 1934D accessory coupled to the spectrofluorometer.

3. Results and discussion

3.1. Characterization of the $[RE(TPC)_3 \cdot (H_2O)_2]$ complexes

The percentages of the rare earth ions (RE^{3+} = Sm, Eu, Gd and Tb) were determined by complexometric titration with EDTA, where the RE-complexes were dissolved in methanol using xylenol orange as indicator. These data together with the results of the elemental analyses of C and H indicate the general formula for the $[RE(TPC)_3 \cdot (H_2O)_2]$ complexes. Their *Anal.* Calc. values are: Sm^{3+}-complex (Sm, 26.48; C, 31.73; H, 2.31. Found: Sm, 26.52; C, 31.69; H, 2.40); Eu^{3+}-complex (Eu, 26.68; C, 31.64; H, 2.30. Found: Eu, 26.65; C, 31.09; H, 2.32); Gd^{3+}-complex (Gd, 27.36; C, 31.34; H, 2.28. Found: Gd, 27.35; C, 31.01; H, 2.30) and Tb-complex (Tb, 27.57; C, 31.25; H, 2.27. Found: Tb, 27.61; C, 30.90; H, 2.37).

The coordination of the ligand to the rare earth ion was investigated comparing the infrared spectra of the complexes with those of the sodium–TPC salt as suggested in [12]. The IR spectrum of the TPC in ionic form presents strong bands around 1388 and 1557 cm^{-1}, which are attributed to the ν_s(C=O) and ν_{as}(C=O) vibrational modes, respectively. On the other hand, the infrared spectra of the RE^{3+}-complexes (Sm, Eu, Tb and Gd) display an additional band at 1512 cm^{-1}, suggesting two coordination forms of TPC to the metal ions. Besides, the spectral data show smaller difference ($\Delta\nu_{(C=O)} = \nu_{as} - \nu_s$) between the stretching frequencies relative to the values for the ionic ligand, suggesting that the TPC ligand is coordinated to the rare earth ion as chelate and bridge forms via oxygen atoms of the carboxylic groups. The infrared spectra also show a very broad band around 3311 cm^{-1} assigned to ν(O–H) confirming the presence of water molecules coordinated to the RE^{3+} ions.

3.2. Structural data of the $[Eu(TPC)_3 \cdot (H_2O)_2]$ complex

Single crystal of the $[Eu(TPC)_3 \cdot (H_2O)_2]$ complex was obtained by dissolving the powder complex in a water:ethanol solvent mixture (1:1, v/v). The crystal started growing up from the mother solution at room temperature (~298 K) during a period of three weeks. No sign of deterioration during storage under ordinary laboratory atmospheric conditions was observed. Crystallographic data for the structure determination of the $[Eu(TPC)_3 \cdot (H_2O)_2]$ complex are listed in Table 1. X-ray data indicate that the Eu^{3+}-complex belongs to the $P2_1/n$ space group in the monoclinic system.

As can be seen in Fig. 1(a) this complex is a dimer with two TPCs acting as a bridging ligand by binding to the Eu(1) and Eu(1A) centers via carboxylate groups by O(4) and O(4A), while other two TPCs are chelated to each metal ion. The crystalline structural data corroborate with the infrared spectroscopy indicating two different coordination modes of the TPC ligand to the europium ion. It is interesting to observe that the dimeric system of the Eu^{3+}–TPC complex has an inversion center of symmetry indicating that the Eu(1) and Eu(1A) centers are in equivalent chemical environments. The distance between Eu(1) and Eu(1A) ions in the dimer is equal to 4.374 Å.

Fig. 1(b) displays a ZORTEP plot of the coordination polyhedron, suggesting a distorted antiprismatic arrangement of the oxygen atoms around the europium ion with point symmetry close to C_{2v}, while Table 2 presents the distances from the Eu(1) center to oxygen atoms in the first coordination sphere. The interatomic distances Eu(1)–O(x) (where x = 1, 2, 3 and 5) for the chelate cyclic groups with an average value of 2.463 Å are larger than those of the bridge groups, which present distances of Eu(1)–O(4) = 2.340 Å and Eu(1)–O(8A) = 2.371 Å. All these results are comparable to the values found in other rare earth complexes with similar coordination mode [25]. On the other hand, the distances from the oxygen atoms of water molecules to the europium ion lie between those of the bidentate and bridge oxygen atoms (Table 2).

Table 1
Crystal data and structure refinement for the europium complex

Empirical formula	$C_{15}H_{13}EuO_8S_3$
Formula weight	569.42
Temperature (K)	293(2)
Wavelength (Å)	0.71073
Crystal system, space group	monoclinic, $P2_1/n$
Unit cell dimensions	
a (Å)	10.042(5)
b (Å)	19.593(5)
c (Å)	11.168(5)
α (°)	90.000(5)
β (°)	116.250(5)
γ (°)	90.000(5)
V (Å^3)	1970.7(14)
Z	4
D_c (g cm^{-3})	1.774
Absorption coefficient (mm^{-1})	3.531
$F(000)$	1012
Limiting indices	$-12 \leqslant h \leqslant 12$
	$-24 \leqslant k \leqslant 0$
	$-13 \leqslant l \leqslant 13$
Reflections collected/unique	7698/3879 [$R_{int} = 0.0785$]
Refinement method	full-matrix least-squares on F^2
Data/restraints/parameters	3879/0/247
Goodness-of-fit on F^2	1.006
Final R indices [$I > 2\ (I)$]	$R_1 = 0.0526$
	$wR_2 = 0.1483$
R indices (all data)	$R_1 = 0.0961$
	$wR_2 = 0.1707$

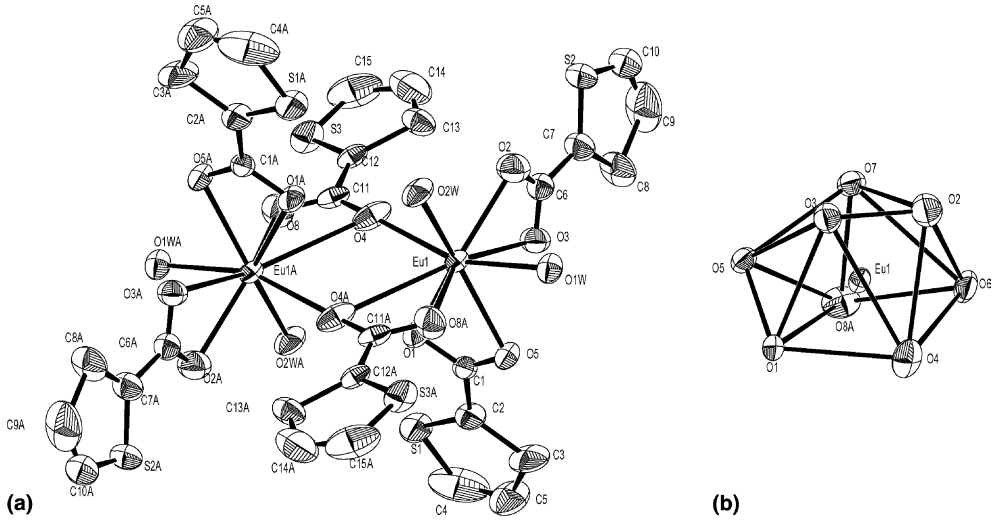

Fig. 1. Structure of the europium complex with the atomic labels: (a) Dimeric form and (b) Distorted polyhedral coordination around the europium ion.

Table 2
Bond lengths (Å) and selected angles (°) around the europium ion

Bond lengths			
Eu(1)–O(1)	2.443(7)	Eu(1)–O(5)	2.495(7)
Eu(1)–O(2)	2.462(8)	Eu(1)–O(6)$_{water}$	2.429(7)
Eu(1)–O(3)	2.450(7)	Eu(1)–O(7)$_{water}$	2.419(6)
Eu(1)–O(4)	2.340(7)	Eu(1)–O(8)	2.371(7)
Bond angles			
O(4)–Eu(1)–O(8)	115.6(3)	O(1)–Eu(1)–O(3)	85.4(2)
O(4)–Eu(1)–O(7)	157.7(3)	O(4)–Eu(1)–O(2)	86.4(3)
O(8)–Eu(1)–O(7)	73.5(3)	O(8)–Eu(1)–O(2)	137.0(3)
O(4)–Eu(1)–O(6)	77.0(2)	O(7)–Eu(1)–O(2)	74.7(3)
O(8)–Eu(1)–O(6)	76.4(3)	O(6)–Eu(1)–O(2)	73.3(3)
O(7)–Eu(1)–O(6)	86.2(2)	O(1)–Eu(1)–O(2)	131.7(3)
O(4)–Eu(1)–O(1)	74.3(3)	O(3)–Eu(1)–O(2)	52.9(2)
O(8)–Eu(1)–O(1)	90.9(3)	O(4)–Eu(1)–O(5)	126.0(2)
O(7)–Eu(1)–O(1)	127.4(2)	O(8)–Eu(1)–O(5)	78.5(2)
O(6)–Eu(1)–O(1)	139.4(2)	O(7)–Eu(1)–O(5)	74.8(2)
O(4)–Eu(1)–O(3)	96.6(3)	O(6)–Eu(1)–O(5)	152.0(2)
O(8)–Eu(1)–O(3)	145.2(3)	O(1)–Eu(1)–O(5)	52.8(2)
O(7)–Eu(1)–O(3)	81.5(2)	O(3)–Eu(1)–O(5)	71.7(2)
O(6)–Eu(1)–O(3)	126.2(3)	O(2)–Eu(1)–O(5)	119.4(2)

3.3. Spectroscopic study

3.3.1. Theoretical intensity parameters

According to the theoretical model developed for the 4f–4f intensities, the calculations to obtain the Ω_λ intensity parameters ($\lambda = 2$, 4 and 6) depend on both the chemical environment and the rare earth ion. They are given by [26]

$$\Omega_\lambda = (2\lambda + 1) \sum_{t,p} \frac{|B_{\lambda \mathrm{tp}}|^2}{(2t+1)}, \tag{1}$$

where the quantities $B_{\lambda \mathrm{tp}}$ are known as the intensity parameters of individual transitions between Stark levels [27,28] and have been expressed by

$$B_{\lambda \mathrm{tp}} = \frac{2}{\Delta E} \langle r^{t+1} \rangle \theta(t,\lambda) \gamma_p^t - \left[\frac{(\lambda+1)(2\lambda+3)}{(2\lambda+1)} \right]^{1/2} \times \langle r^\lambda \rangle (1-\sigma_\lambda) \langle 3 \| C^{(\lambda)} \| 3 \rangle \Gamma_p^t \delta_{t,\lambda+1}, \tag{2}$$

where ΔE is the energy difference between the barycenters of the excited $4f^5 5d$ and ground $4f^6$ configurations, $\langle r^\lambda \rangle$ is a radial expectation value, $\theta(t,\lambda)$ is a numerical factor, σ_λ is a shielding factor and $C^{(\lambda)}$ is a Racah tensor operator of rank λ. The sums-over-ligands γ_p^t and Γ_p^t contain the dependence on the coordination geometry and on the nature of the chemical environment around the rare earth ion. In our treatment the latter is given by

$$\Gamma_p^t = \left(\frac{4\pi}{2t+1}\right)^{1/2} \sum_j \frac{\alpha_j}{R_j^{t+1}} Y_p^{t*}(\Omega_j), \quad (3)$$

where α_j is the isotropic polarizability of the jth ligand atom, or group of atoms, at position $\vec{R}_j$, and Y_p^t is a spherical harmonic of rank t. The ligand field parameters, γ_p^t, are those given by simple overlap model (SOM) [26]

$$\gamma_p^t = \left(\frac{4\pi}{2t+1}\right)^{1/2} \sum_j \rho_j (2\beta_j)^{t+1} \frac{g_j e^2}{R_j^{t+1}} Y_p^{t*}(\Omega_j), \quad (4)$$

where ρ_j is the magnitude of the total overlap between 4f and ligand wavefunctions and $\beta_j = 1/(1+\rho_j)$ in our case. The charge factors g_j can be treated as parameters, which no longer have to be given by the valence of the ligand atoms [26–28].

3.3.2. Gd^{3+}–TPC complex

In order to obtain the structure of energy states of the 2-thiophenecarboxylate ligand, we have studied the photophysical properties of $[Gd(TPC)_3 \cdot (H_2O)_2]$ complex by emission spectra, at 77 K. In this case, the energy of the triplet state (T) arising from the organic ligand is obtained using the Gd^{3+} ion, owing to the large energy gap ($\sim$32,000 cm^{-1}) between the $^8S_{7/2}$ ground state and first $^6P_{7/2}$ excited state [29]. In this case the trivalent gadolinium ion cannot accept any energy from the first excited triplet state of the TPC ligand. Fig. 2(a) shows the excitation spectrum of the gadolinium complex, recorded in the spectral range from 250 to 420 nm at 77 K, that displays two broad bands with maxima at 280 and 320 nm which can be attributed to ligand centered $S_0 \rightarrow S_1$ (π, π^* and n, π^*) transitions. The emission spectrum of this complex (Fig. 2(b)) recorded from 360 up to 625 nm, by monitoring the excitation at 320 nm ($S_0 \rightarrow S_1$ transition), shows strong bands with maxima at 408 and 437 nm which are an image in a mirror plane of those in the excitation spectrum. A broad band with a maximum around 520 nm that overlaps the former is also observed. In the time-resolved spectra (figure not shown) the intensities of the two bands (around 408 and 437 nm) decrease very fast as the flash delay is increased (0.002 ms), while the band at 520 nm is moderately altered. These results indicate that the bands in higher energies can be attributed to the fluorescence due to the $S_1(\pi, \pi^*$ and $n, \pi^*) \rightarrow S_0$ transitions centered in the ligand.

The luminescence decay curve of the Gd–TPC complex was recorded at 77 K under excitation at 320 nm and emission monitored at 520 nm. The value of the lifetime of the triplet state ($\tau_T = 3.8$ ms) is larger, corroborating with the time-resolved spectra and indicating that the broad band at lower energy arises from $T(\pi, \pi^*$ and $n, \pi^*) \rightarrow S_0$ transitions. The triplet state was taken as the shortest wavelength from the phosphorescence band in the time-resolved spectra due to 0–0 transition with the energy level position around 22,624 cm^{-1} [30–32].

3.3.3. Eu^{3+}–TPC complex

The excitation spectrum of the $[Eu(TPC)_3 \cdot (H_2O)_2]$ complex was recorded in the spectral range from 250 up to 590 nm with the emission monitored on the hypersensitive

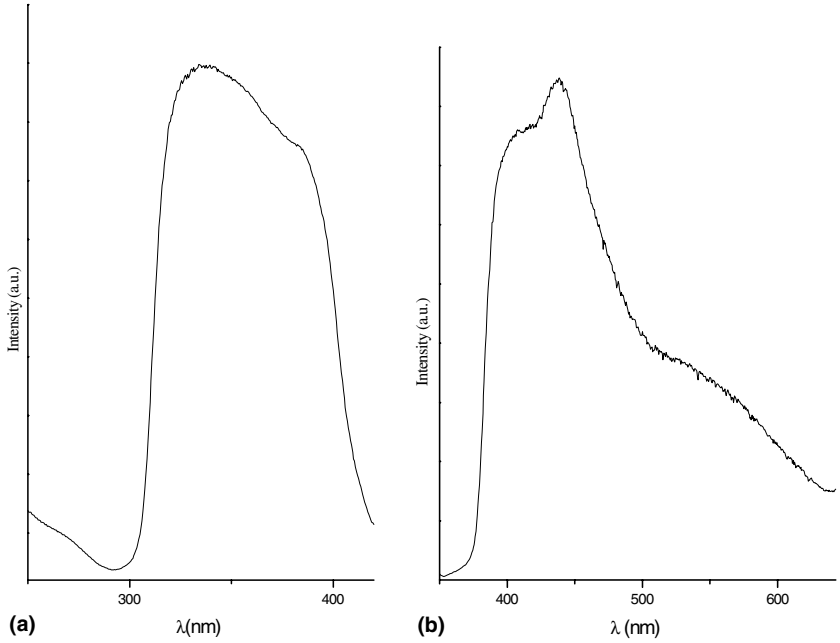

Fig. 2. Luminescence spectra of the $[Gd(TPC)_3 \cdot (H_2O)_2]$ complex in solid state, at 77 K: (a) excitation spectrum under emission on the $T \rightarrow S_0$ transition centered on the TPC ligand, at 425 nm and (b) phosphorescence spectrum monitored on the $S_0 \rightarrow S_1$ transition at 310 nm.

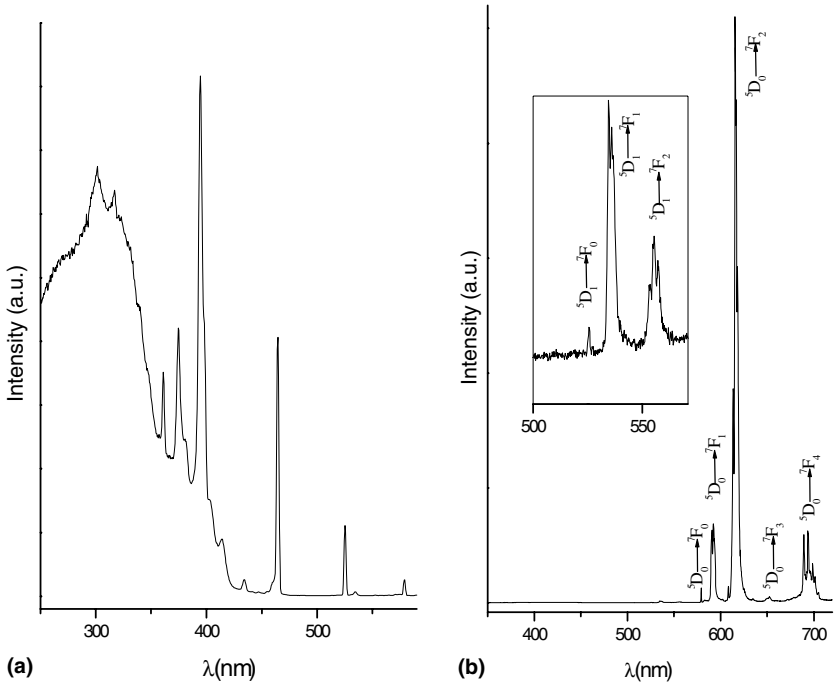

Fig. 3. Luminescence spectra of the $[Eu(TPC)_3 \cdot (H_2O)_2]$ complex in solid state, at 77 K: (a) excitation spectrum with emission monitored on the hypersensitive $^5D_0 \rightarrow {}^7F_2$ transition of the Eu^{3+} ion, at 612 nm and (b) emission spectrum monitored on the TPC ligand band, at 310 nm.

$^5D_0 \rightarrow {}^7F_2$ transition at 612 nm (Fig. 3(a)). This spectrum displays an intense strong band from 300 to 420 nm that is attributed to the TPC, indicating that this ligand is a good sensitizer for the Eu^{3+} luminescence. In addition, several narrow bands are also observed which are assigned to $4f^6$-intraconfigurational transitions from the ground state $^7F_0$ to the following excited state of the europium ion (in nm): $^5G_6$ (361), $^5H_4$ (374), $^5L_6$ (394), $^5D_2$ (464), $^5D_1$ (532) and $^5D_0$ (578).

Fig. 3(b) shows the emission spectrum of the Eu–TPC-complex in solid state recorded in the range of 420–720 nm under excitation on the singlet state of the TPC ligand at 310 nm, at 77 K. The emission data (Fig. 3(b)) show intense narrow bands from the $^5D_0 \rightarrow {}^7F_J$ transitions (where $J = 0$–4) dominated by the hypersensitive $^5D_0 \rightarrow {}^7F_2$ transition around 612 nm. The presence of the $^5D_0 \rightarrow {}^7F_0$ transition indicates that the europium ion is located in a symmetry site of the type C_s, C_n or C_{nv}. Besides, it is observed that the $^5D_0 \rightarrow {}^7F_J$ transitions ($J = 0$–4) are split in their respective maximum number of $(2J + 1)$-components (Table 3), indicating that the Eu^{3+} ions have the same chemical environment, in agreement with the structural data reported previously. Also are noted for the Eu-complex (Fig. 3(b), inset) the low intensity lines around 526, 535 and 550 nm, corresponding to the $^5D_1 \rightarrow {}^7F_0$, $^7F_1$ and $^7F_2$ transitions, respectively. The emission spectrum of the $[Eu(TPC)_3 \cdot (H_2O)_2]$ complex shows a ligand-field splitting of the $^5D_0 \rightarrow {}^7F_J$ transitions consistent with a C_{2v} site symmetry for the Eu^{3+} ion, which is in accordance with the single crystal X-ray diffraction data, that suggested a distorted antiprismatic arrangement of oxygen atoms around the Eu^{3+} ions.

One of the interesting aspects in this system is that the high luminescence intensity bands from the ligand, recorded in the spectral range from 350 to 650 nm for the Gd-complex (Fig. 2(b)), are not observed in the Eu-complex (Fig. 3(b)), indicating that the TPC ligand acts as an efficient luminescence sensitizer for the europium compound. Since the Gd-complex exhibits fluorescence due to $S_1(\pi, \pi^*$ and $n, \pi^*) \rightarrow S_0$ transitions of the TPC ligand which is absent in the $[Eu(TPC)_3 \cdot (H_2O)_2]$ complex, the intramolecular energy transfer probably can occur from the singlet states $S_1(\pi, \pi^*)$ and $S_1(n, \pi^*)$ to the excited $^5D_3$ or $^5L_6$ states of the metal ion which are 2667 and 1286 cm^{-1}, respectively, lesser energetic than the formers.

In order to determine the emission quantum efficiency (η) of the $^5D_0$ emitting level in $[Eu(TPC)_3 \cdot (H_2O)_2]$ an emission spectrum of this compound was recorded under excitation at 394 nm (figure not shown). This spectrum showed the same profile as the one recorded under excitation on the ligand band. The luminescence decay curve of the $^5D_0$ emitting level recorded under excitation at 394 nm and emission monitored at 612 nm exhibits a single exponential behavior.

Based on the emission spectrum and lifetime of the $^5D_0$ emitting level ($\tau = 0.33$ ms) the emission quantum efficiency (η) of the europium ion in the $[Eu(TPC)_3 \cdot (H_2O)_2]$ compound was determined. First the emission

Table 3
Energies of $^4G_{5/2} \rightarrow {}^6H_J$ (Sm^{3+}), $^5D_0 \rightarrow {}^7F_J$ (Eu^{3+}) and $^5D_4 \rightarrow {}^7F_J$ (Tb^{3+}) transitions (in cm^{-1}) observed in the emission spectra of the [RE(TPC)$_3$(H$_2$O)$_2$] complexes, at 77 K

[Eu(TPC)$_3 \cdot$(H$_2$O)$_2$]		[Sm(TPC)$_3 \cdot$(H$_2$O)$_2$]		[Tb(TPC)$_3 \cdot$(H$_2$O)$_2$]	
$^5D_0 \rightarrow {}^7F_0$	17265	$^4G_{5/2} \rightarrow {}^6H_{5/2}$	17832	$^5D_4 \rightarrow {}^7F_6$	20568
			17762		20492
$^5D_0 \rightarrow {}^7F_1$	16949				20425
	16886	$^4G_{5/2} \rightarrow {}^6H_{7/2}$	16869		20259
	16858		16824		
			16762	$^5D_4 \rightarrow {}^7F_5$	18443
$^5D_0 \rightarrow {}^7F_2$	16442		16650		18409
	16306		16589		18376
	16244		16545		18315
	16218				18182
	16176	$^4G_{5/2} \rightarrow {}^6H_{9/2}$	15605		
			15571	$^5D_4 \rightarrow {}^7F_4$	17224
$^5D_0 \rightarrow {}^7F_3$	15399		15489		17170
	15380		15432		17147
	15366		15375		17071
	15342				17030
	15328	$^4G_{5/2} \rightarrow {}^6H_{11/2}$	14306		16966
	15295		14237		16852
	15263		14148		
			14096	$^5D_4 \rightarrow {}^7F_3$	16160
$^5D_0 \rightarrow {}^7F_4$	14611		14049		16093
	14505		13998		16057
	14413				16036
	14368				
	14355			$^5D_4 \rightarrow {}^7F_2$	15509
	14310				15461
	14261				15370
	14188				15267
				$^5D_4 \rightarrow {}^7F_1$	15002
					14934
				$^5D_4 \rightarrow {}^7F_0$	14719

coefficients A_{02} and A_{04} of the forced electric dipole transitions $^5D_0 \rightarrow {}^7F_2$ and $^5D_0 \rightarrow {}^7F_4$, respectively, were calculated taking the magnetic dipole transition $^5D_0 \rightarrow {}^7F_1$ as the standard since this transition is practically insensitive to the chemical environment around the europium ion. By the relation between the lifetime of the emitting state and total decay rate, $A_{\text{tot}} = \frac{1}{\tau} = A_{\text{rad}} + A_{\text{nrad}}$, where A_{rad} and A_{nrad} are the radiative and non-radiative rates, respectively, the η value can be calculated by the following equation:

$$\eta = \frac{A_{\text{rad}}}{A_{\text{rad}} + A_{\text{nrad}}}. \tag{5}$$

The low value of $\eta \sim 21.4\%$ calculated for [Eu(TPC)$_3 \cdot$(H$_2$O)$_2$] reflects the large value of the non-radiative rate ($A_{\text{nrad}} = 2376\ s^{-1}$) due to the luminescence quenching of the $^5D_0$ emitting level by OH oscillators of the two water molecules in the first coordination sphere [2].

The experimental intensity parameters (Ω_2 and Ω_4) for the Eu–TPC-complex were determined from the spectral data of the $^5D_0 \rightarrow {}^7F_2$ and $^5D_0 \rightarrow {}^7F_4$ transitions, respectively, according to the following expression [26]:

$$\Omega_\lambda = \frac{4e^2\omega^3 A_{0\lambda}}{3\hbar c^3 \chi \left\langle {}^7F_\lambda \| U^{(\lambda)} \| {}^5D_0 \right\rangle^2}, \tag{6}$$

where $A_{0\lambda}$ are the coefficients of spontaneous emission, χ is the Lorentz local field correction term that is given by $\chi = n(n^2+2)^2/9$ with the refraction index $n = 1.5$ and $\langle {}^7F_\lambda \| U^{(\lambda)} \| {}^5D_0 \rangle^2$ are the squared reduced matrix elements whose values are 0.0032 and 0.0023 for $\lambda = 2$ and 4, respectively.

The theoretical (semi-empirical) intensity parameters Ω_λ (Section 3.3.1) were calculated from the X-ray structural data. Spherical coordinates that were used in this calculation are given in Table 4. The polarizability α (Eq. (3)) and charge factor g (Eq. (4)) were treated as freely varying parameters by assuming two types of oxygen ligating atoms, one for the TPC ligand and another for the water molecule. The best values found were $g(\text{TPC}) = 0.5$, $g(\text{H}_2\text{O}) = 0.6$, $\alpha(\text{TPC}) = 2.0$ Å^3 and $\alpha(\text{H}_2\text{O}) = 4.4$ Å^3. An important feature of Eq. (2) is that the first term in the right-hand side corresponds to the forced electric dipole mechanism ($\Omega_\lambda^{e.d}$, $\alpha_j = 0$), as expressed by the average energy denominator method, and

Table 4
Spherical coordinates of the eight oxygen atoms bonded to the Eu^{3+} ion in the $[Eu(TPC)_3(H_2O)_2]$ compound

$[Eu(TPC)_3(H_2O)_2]$	R (Å)	θ	ϕ
TPC oxygen	2.443	115.17	302.43
	2.462	34.77	52.05
	2.451	87.63	48.85
	2.340	82.97	325.82
	2.496	145.23	356.45
	2.369	108.05	80.50
H_2O oxygen	2.430	38.74	43.69
	2.419	74.71	326.98

the second term corresponds to the dynamic coupling mechanism ($\Omega_\lambda^{c.d}$, $g_j = 0$) within the point dipole isotropic ligand polarizability approximation. The results, which are quite satisfactory in comparison with the experimental values, are presented in Table 5. This corroborates the reliability of the theoretical model. For the sake of comparison the values for the $Eu(TTA)_3 \cdot (H_2O)_2$ complex [18] are also presented.

The $[Eu(TPC)_3 \cdot (H_2O)_2]$ complex presents values of $\Omega_2^{d.c} = 18.3$ and $\Omega_4^{d.c} = 7.3$, which are much larger than $\Omega_2^{e.d} = 0.48$ and $\Omega_4^{e.d} = 0.06$ (in units of 10^{-20} cm^2), indicating that the Eu^{3+} ion is in chemical environment highly polarizable, but less polarizable than in the case of the complex with the TTA ligand. The dynamic coupling mechanism is, therefore, dominant, also suggesting a higher covalent contribution to the ligand–rare earth ion bonding as compared to the bonding in ionic environments containing fluoride ligands.

Table 5
Experimental and theoretical intensity parameters (Ω_λ) for the europium complexes

Complexes		Ω_2 (10^{-20} cm^2)	Ω_4 (10^{-20} cm^2)
$[Eu(TPC)_3(H_2O)_2]$	Experimental	15.8	8.2
	Theoretical	16.9	6.4
$[Eu(TTA)_3(H_2O)_2]$[a]	Experimental	33.0	4.6
	Theoretical	19.8	4.7

[a] Ref. [18].

3.3.4. Tb^{3+}–TPC complex

The $[Tb(TPC)_3 \cdot (H_2O)_2]$ complex exhibits a highly intense green color under UV excitation. The excitation spectrum (Fig. 4(a)) with emission monitored on the $^5D_4 \rightarrow {}^7F_5$ transition (542 nm) shows intense broad bands in the range from 250 to 330 nm, attributed to the singlet states, similar to the europium complex. The narrow bands arising from the intraconfigurational transitions: $^7F_6 \rightarrow {}^5L_6$ (339 nm), $^7F_6 \rightarrow {}^5L_9$ (350 nm), $^7F_6 \rightarrow {}^5L_{10}$ (369 nm), $^7F_6 \rightarrow {}^5G_6$ (376 nm), $^7F_6 \rightarrow {}^5D_3$ (380 nm) and $^7F_6 \rightarrow {}^5D_4$ (488 nm) are also observed. As can be seen in Fig. 4(a), the ligand bands are much more intense than those from the rare earth ion, indicating that indirect excitation processes are efficient in the Tb–TPC complex.

Upon excitation through the singlet state of the TPC ligand, at 311 nm, the emission spectrum of $[Tb(TPC)_3 \cdot (H_2O)_2]$ at 77 K (Fig. 4(b)) does not display the broad band from the ligand in the range of 380–480 nm, showing an efficiency energy transfer from the ligand states to the emitting $^5D_4$ level of the terbium ion. The compound was also excited on the $^7F_6 \rightarrow {}^5L_9$ transition (350 nm), but no difference in the profile of the 4f–4f transitions was observed. The luminescence decay curve of the $^5D_4$ emitting level was obtained by excitation on

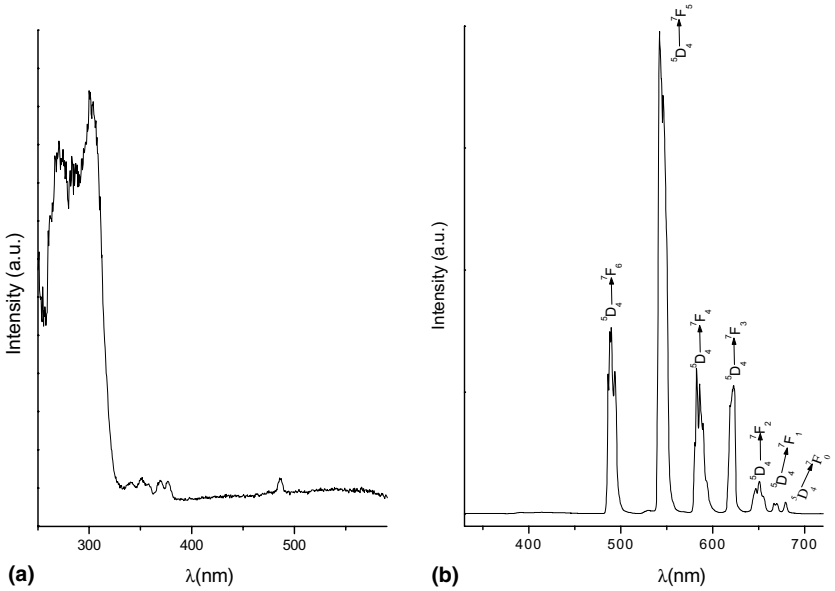

Fig. 4. Luminescence spectra of the $[Tb(TPC)_3 \cdot (H_2O)_2]$ complex in solid state, at 77 K: (a) excitation spectrum under emission on the hypersensitive $^5D_4 \rightarrow {}^7F_5$ transition of the Tb^{3+} ion, at 542 nm and (b) emission spectrum monitored on the TPC ligand band, at 310 nm.

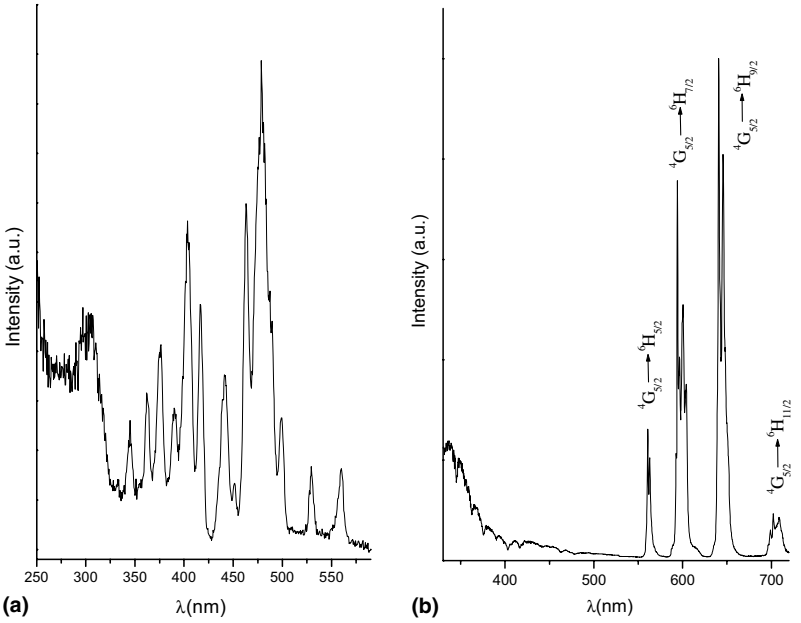

Fig. 5. Luminescence spectra of the $[Sm(TPC)_3 \cdot (H_2O)_2]$ complex in solid state, at 77 K: (a) excitation spectrum under emission on the $^4G_{5/2} \rightarrow {}^6H_{9/2}$ transition of the Sm^{3+} ion, at 642 nm and (b) emission spectrum monitored on the TPC ligand band, at 310 nm.

the $^7F_6 \rightarrow {}^5L_9$ transition and emission monitored at the $^5D_4 \rightarrow {}^7F_5$ transition. This curve has a single exponential behavior with a lifetime (τ) equal to 0.23 ms.

3.3.5. Sm^{3+}–TPC complex

As shown in Fig. 5(a), the excitation spectrum of the samarium complex at 77 K shows a broad band that covers the entire 300–340 nm region with a maximum around 305 nm. The spectrum also presents several narrow bands arising from the intraconfigurational transitions from the $^6H_{5/2}$ ground state to the following levels (in nm): $^4H_{9/2}$ (345), $^4F_{9/2}$ (363), $^4L_{17/2}$ (375), $^4H_{11/2}$ (390), $^4F_{7/2}$ (403), $^4M_{19/2}$ (417), $^4I_{15/2}$ (442), $^4F_{3/2}(1)$ (452), $^4I_{13/2}$ (463), $^4I_{11/2}$ (478), $^4G_{7/2}$ (499), $^4F_{3/2}(2)$ (530) and $^4G_{5/2}$ (560). As can be observed the $^4G_{5/2} \rightarrow {}^4I_{11/2}$ (478 nm) transition exhibits a higher intensity than the ligand band, indicating that in this case the indirect excitation is less efficient than the direct excitation in the $^4G_{5/2} \rightarrow {}^4I_{11/2}$ transition.

In contrast to the europium and terbium complexes, which show high luminescence intensity, the $[Sm(TPC)_3 \cdot (H_2O)_2]$ complex displays a characteristic orange color presenting only a weak luminescence intensity under UV excitation. The emission spectrum of $[Sm(TPC)_3 \cdot (H_2O)_2]$ at 77 K upon excitation at 305 nm is given in Fig. 5(b). In this spectrum, the broad band is attributed to the fluorescence from the TPC ligand in the range from 380 to 460 nm. Besides, some dips are detectable inside the broad bands that are attributed to the absorption lines (in nm): $^6H_{5/2} \rightarrow {}^4H_{9/2}$ (345), $^4F_{9/2}$ (363), $^4L_{17/2}$ (375), $^4H_{11/2}$ (390), $^4F_{7/2}$ (403), $^4M_{19/2}$ (417), $^4I_{13/2}$ (463) and $^4I_{11/2}$ (478). Additionally, sharp bands characteristic of the $^4G_{5/2} \rightarrow {}^6H_J$ transitions ($J = 5/2$, 7/2, 9/2 and 11/2), where the hypersensitive $^4G_{5/2} \rightarrow {}^6H_{9/2}$ transition is dominant, are also observed. Table 3 presents the ligand-field splitting of the $^4G_{5/2} \rightarrow {}^6H_J$ transitions. The observed maximum number of Stark transitions is consistent with the Sm^{3+} ion in a chemical environment with low symmetry.

From the emission spectrum (Fig. 5(b)) the η_{Sm} intensity parameter, which is the ratio between the intensities of the $^4G_{5/2} \rightarrow {}^6H_{9/2}$ and $^4G_{5/2} \rightarrow {}^6H_{5/2}$ transitions, was determined [7]. The transition $^4G_{5/2} \rightarrow {}^6H_{5/2}$ (around 560 nm) was taken as the reference due to its predominant magnetic dipole character ($\Delta J = 0$). On the other hand, the $^4G_{5/2} \rightarrow {}^6H_{9/2}$ transition is magnetic-dipole forbidden and electric-dipole allowed. The value of the experimental intensity parameter $\eta_{Sm} = 4.5$ suggests that the samarium ion is in a moderately polarizable chemical environment when compared with the $[Sm(TTA)_3 \cdot (H_2O)_2]$ complex ($\eta_{Sm} = 8.9$) reported in [20].

Comparing the luminescence properties of the rare earth compounds it is observed that the TPC to the metal ion energy transfer processes is more efficient in the case of Eu^{3+} and Tb^{3+} than in the case of Sm^{3+}. This can be explained based on the more favorable energy mismatch conditions in the case of Eu^{3+} and Tb^{3+}.

4. Conclusions

The synthesis, characterization and crystalline structure of the $[Eu(TPC)_3 \cdot (H_2O)_2]$ complex indicated that the TPC ligand chelates to the rare earth ions via the carboxylic oxygen donors and it also functions as a bridge ligand in the formation of a dimeric complex

where two identical Eu^{3+} centers are involved. The coordination polyhedron can be described as a distorted square antiprism, with site symmetry close to C_{2v}.

A rather weak intersystem crossing (singlet to triplet) in the TPC ligand is suggested by the high luminescence intensity of the bands arising from the allowed $S_1(\pi,\pi^*$ and $n,\pi^*) \rightarrow S_0$ transitions in the emission spectrum of the Gd^{3+}-complex, at 77 K. The absence of these bands in the emission spectrum of the europium and terbium complexes indicates that probably the S_1 state of the TPC ligand plays a role in the energy transfer from the ligand to the rare earth ions.

The ligand-field splitting observed from the $^5D_0 \rightarrow {}^7F_J$ transitions of the Eu^{3+} ion ($J = 0$–4) indicates the presence of a unique chemical environment around the metal ion, which is consistent with the structural data. The theoretical (semi-empirical) values of the intensity parameters, calculated from the structural data, are in good agreement with the experimental values, showing the reliability of the theoretical model. These values also indicate that the rare earth ion is in a chemical environment highly polarizable, though to a less degree than in the case of the $Eu(TTA)_3 \cdot (H_2O)_2$ complex as presented in Table 5.

The luminescence data suggest that the TPC ligand can activate efficiently the luminescence of the Eu^{3+} and Tb^{3+} ions. The substitution of two water molecules by some organic ligand (example: sulfoxides, amides, heterocyclics, etc.) can increase the emission quantum efficiency, making the Eu–TPC-complex a potential candidate as emitter in photonic systems.

Acknowledgements

This research is supported by grants from the Fundação de Amparo à Pesquisa do Estado de São Paulo (FAPESP) and the Conselho Nacional de Desenvolvimento Científico e Tecnológico (CNPq-RENAMI).

References

[1] I.A. Hemmilä, Application of Fluorescence in Immunoassays, Wiley, New York, 1991.
[2] J.-C.G. Bünzli, G.R. Choppin (Eds.), Lanthanide Probes in Life, Chemical and Earth Sciences – Theory and Practice, Elsevier, Amsterdam, 1989.
[3] J. Kido, Y. Okamoto, Chem. Rev. 102 (2002) 2357.
[4] R. Reyes, E.N. Hering, M. Cremona, C.F.B. Silva, H.F. Brito, C.A. Achete, Thin Solid Films 420–421 (2002) 23.
[5] N. Sabatini, M. Guardigli, J.M. Lehn, Coord. Chem. Rev. 123 (1993) 201.
[6] S. Salama, F.S. Richardson, Inorg. Chem. 19 (1980) 629.
[7] Z.M. Wang, L.J. Van de Burgt, G.R. Choppin, Inorg. Chim. Acta 310 (2000) 248.
[8] L.J. Yuan, J. Li, K.L. Zhang, J.T. Sun, Spectrosc. Spect. Anal. 20 (2000) 878.
[9] L.J. Yuan, J.T. Sun, Q.G. Wang, K.L. Zhang, Spectrosc. Lett. 32 (1999) 867.
[10] J.C.G. Bunzli, L.J. Charboniere, R.F. Ziessel, J. Chem. Soc., Dalton Trans. 12 (2000) 1917.
[11] M. Latva, J. Kankare, J. Coord. Chem. 43 (1998) 121.
[12] G.B. Deacon, R.J. Phillips, Coord. Chem. Rev. 33 (1980) 251.
[13] M.J. Amphlett, A.G. Callely, Helv. Chim. Acta 54 (1971) 2214.
[14] S.C. Dixit, R. Sharan, R.N. Kapoor, Inorg. Chim. Acta 145 (1988) 39.
[15] V.N. Gogte, L.G. Shah, B.D. Tilak, K.N. Gadekar, M.B. Sahasrab, Tetrahedron 23 (1967) 2437.
[16] S.S. Sandhu, R.S. Sandhu, J.N. Kumaria, J. Singh, N.S. Sekhon, J. Indian Chem. Soc. 53 (1975) 114.
[17] M. Singh, R. Singh, S.S. Sandhu, J. Indian Chem. Soc. 53 (1976) 1226.
[18] O.L. Malta, H.F. Brito, J.F.S. Menezes, F.R. Gonçalves e Silva, S. Alves Jr., F.S. Farias Jr., A.V.M. de Andrade, J. Lumin. 75 (1997) 255.
[19] F.S. Richardson, Chem. Rev. 82 (1982) 541.
[20] H.F. Brito, O.L. Malta, M.C.F.C. Felinto, E.E.S. Teotonio, J.F.S. Menezes, C.F.B. Silva, C.S. Tomiyama, C.A.A. Carvalho, J. Alloys Compd. 344 (2002) 293.
[21] G. Zucchi, R. Scopelliti, J.C.G. Bünzli, J. Chem. Soc., Dalton Trans. 13 (2001) 1976.
[22] S.J. Lyle, M.M. Rahman, Talanta 10 (1963) 1177.
[23] G.M. Sheldrick, SHELXL97, University of Göttingen, Germany, 1997.
[24] L. Zsolnai, ZORTEP, University of Heidelberg, Germany, 1995.
[25] A. Ouchi, Y. Suzuki, Y. Ohki, Y. Koizumi, Coord. Chem. Rev. 92 (1998) 29.
[26] G.F. de Sá, O.L. Malta, C.M. Donegá, A.M. Simas, R.L. Longo, P.A. Santa-Cruz, E.F. da Silva Jr., Coord. Chem. Rev. 196 (2000) 165.
[27] O.L. Malta, S.J.L. Ribeiro, M. Faucher, P. Porcher, J. Phys. Chem. Solids 52 (1991) 587.
[28] O.L. Malta, M.A. Couto dos Santos, L.C. Thompson, N.K. Ito, J. Lumin. 69 (1996) 77.
[29] H.F. Brito, G.K. Liu, J. Chem. Phys. 112 (2000) 4334.
[30] W.T. Carnall, G.L. Goodman, K. Rajnak, R.S. Rana, J. Chem. Phys. 90 (1989) 3443.
[31] H.R. Mürner, E. Chassat, R.P. Thummel, J.C.G. Bünzli, J. Chem. Soc., Dalton Trans. 16 (2000) 2809.
[32] F.J. Steemers, W. Verboom, D.N. Reinhout, E.B. Vandertol, J.W. Verhoeven, J. Am. Chem. Soc. 117 (1995) 9408.